Progress In Electromagnetics Research Letters, Vol. 84, 39–46, 2019

Multi-Band Printed Antenna for Portable Wireless Communication Applications

Nazih Khaddaj Mallat[1, *] and Amjad Iqbal[2]

Abstract—A compact, triple-band (WiMAX, WLAN and X-Band uplink satellite communication) monopole antenna is reported in this paper. The geometry of the proposed antenna consists of a pentagon-shaped patch along with symmetrical hook-shaped resonators and one vertical slot. The reported antenna works at three unique frequencies centered at 3.5 GHz, 5.4 GHz, and 8 GHz, covering absolute bandwidth of 900 MHz (3.2–4.1 GHz), 800 MHz (5.1–5.9 GHz), and 1.6 GHz (7.3–8.9 GHz), respectively. This antenna possesses good gain and high efficiency at all operating bands. The presented antenna has simulated gain (efficiency) of 4 dBi (78%), 4.2 dBi (79.95%), and 4.2 dBi (85.8%) at 3.5, 5.4, and 8 GHz, respectively. The operating bands of the presented antenna can be tuned independently by varying certain correlated parameters. All the simulations are carried out using High Frequency Structure Simulator (HFSS 13.0). The hardware of the simulated antenna is successfully constructed and tested for validation of simulation results. A reasonable match between the simulated and measured results is observed at the operating bands.

1. INTRODUCTION

Recently, multi-band antennas for multiple applications have received huge attention from researchers due to their efficient utilization of frequency spectrum. The need for one antenna which can cover multiple application bands is always desirable in a modern wireless communication system. Antennas having independently controllable bands have gained much consideration due to the scarcity of the radio frequency spectrum. Microstrip patch antenna is a competitive candidate to be used in wireless communication due to its many advantages over other antennas such as light weight, easy fabrication, and easy production of multiple bands [1, 2].

Various approaches have been adopted for designing multiple band antennas. In [1], symmetrical meandered strips resonators are connected to the top edge of a rectangular patch antenna for generating multiple bands. In [3], two symmetrical strips connected to a slotted-triangular patch antenna produce multiple resonant frequencies (WLAN and WiMAX). A simple antenna with E- and L-shaped radiators is reported in [4] for generating dual bands for WLAN applications. An efficient multiband antenna is reported in [5] in which artificial magnetic conductor is used for gain enhancement while slots in the main radiator produce multiple bands. In [6], a fan-shaped radiator along with a parasitic circular patch produces three distinct resonant bands at WLAN and WiMAX ranges. A miniaturized multiband antenna operating at WLAN and WiMAX bands is reported in [7]. The reported antenna produces distinct resonant frequencies while the defected ground structure enhances the impedance bandwidth. In [8 9], switching components such as lumped elements are utilized for single/dual-band operation of the antenna. Multiband resonant frequencies have been obtained by using U-shaped slot in the main radiating [10] and utilizing c-shaped radiator [11]. A flower-shaped antenna along with

Received 25 February 2019, Accepted 30 April 2019, Scheduled 8 May 2019
* Corresponding author: Nazih Khaddaj Mallat (nazih.mallat@aau.ac.ae).
[1] College of Engineering, Al Ain University of Science and Technology, Al Ain, United Arab Emirates (UAE). [2] Centre for Wireless Technology (CWT), Faculty of Engineering, Multimedia University, Malaysia.

a split ring resonator, operating at multiple bands is reported in [12]. Multiband operation in the reported antenna is incorporated by etching U-shaped and H-shaped slots in the radiating elements while miniaturization is achieved by the defected ground structure. A rectangular dielectric resonator antenna with a combination of the radiating slot is used for multiple band operation in [13]. The reported antennas [1–13] operate well at the resonant frequencies; however, the modern wireless communication system requires components with characteristics of independent resonance control.

A single band pentagon-shaped patch antenna, modified with loading slots and symmetrical hook-shaped resonators for additional frequency bands, is presented in this paper. The proposed antenna works at three dissimilar frequencies with good gain and high efficiency at each operating band. Additionally, the resonant frequencies of the antenna can be independently controlled for efficient frequency spectral utilization.

2. ANTENNA DESIGN

The designed antenna's top, bottom, and side views are illustrated in Figs. 1(a), 1(b), and 1(c), respectively. The proposed antenna is designed on a 1.6 mm thicker commercially available substrate of FR-4 having $\epsilon_r = 4.4$. The overall dimensions of the proposed antenna are $18\times35\times1.6\,\text{mm}^3$. The main radiating element of the antenna is a pentagon-shaped patch which is excited with a $50\,\Omega$ (3 mm) microstrip transmission line. The pentagon-shaped patch has a vertical slot at the lower side while symmetrical hook-shaped resonators are attached to the upper side. A truncated ground is designed on the back of the substrate.

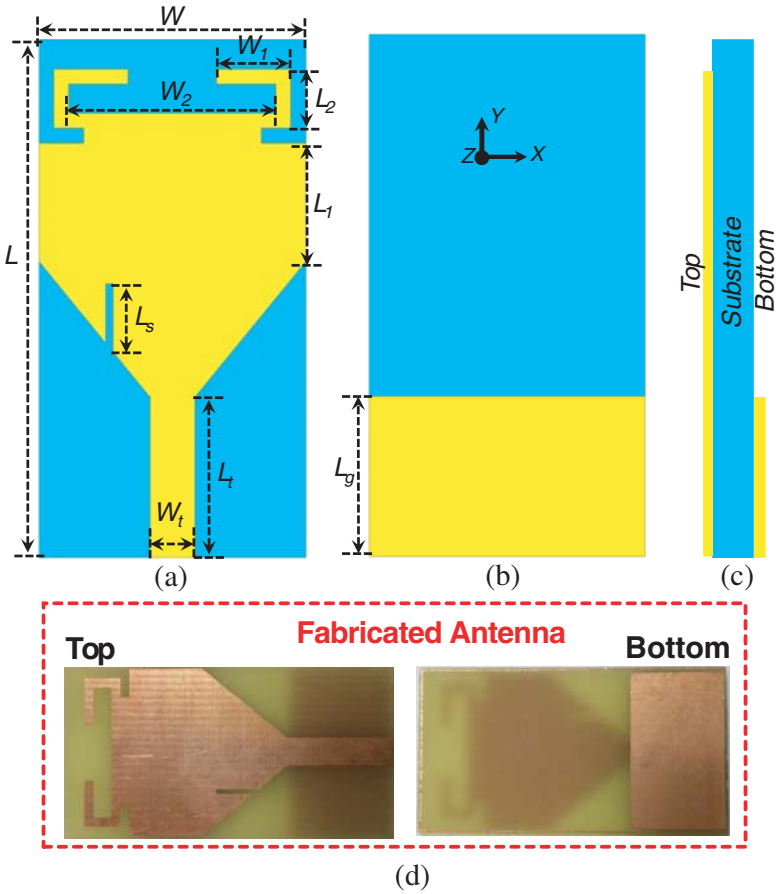

Figure 1. Proposed Antenna (a) Top view ($L = 35\,\text{mm}$, $W = 18\,\text{mm}$, $W_t = 3\,\text{mm}$, $L_t = 10.83\,\text{mm}$, $L_s = 4.6\,\text{mm}$, $L_1 = 8\,\text{mm}$, $L_2 = 4\,\text{mm}$, $W_1 = 5\,\text{mm}$, $W_2 = 14\,\text{mm}$), (b) Bottom view ($L_g = 10.75\,\text{mm}$), and (c) Side view.

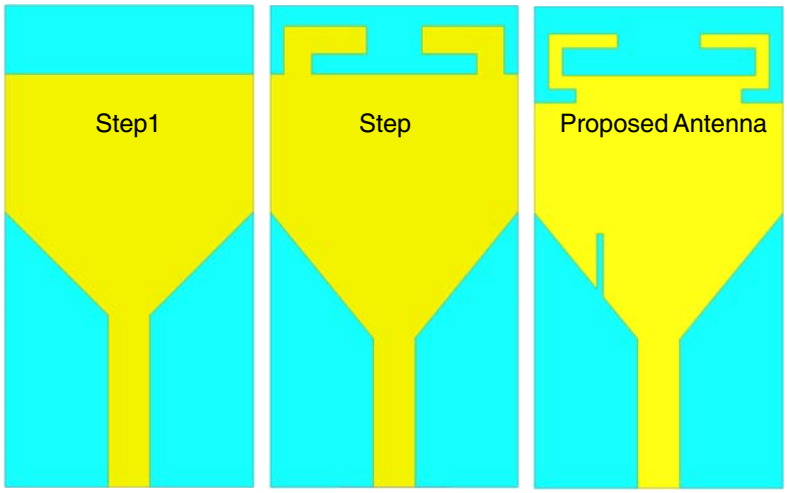

Figure 2. Designing steps of the proposed antenna.

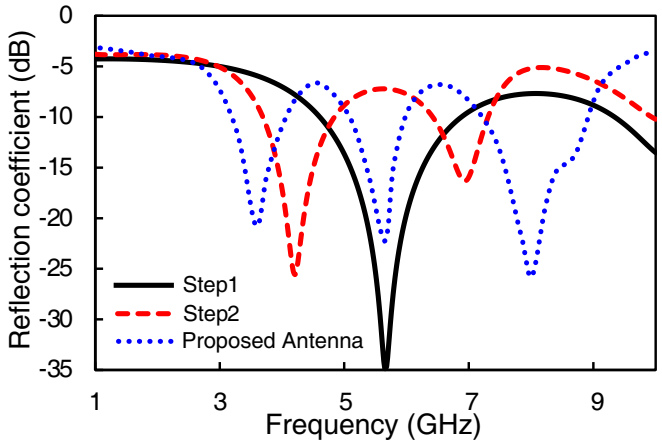

Figure 3. Reflection coefficient of the antenna at each designing step.

The iterative design procedure of the proposed antenna is shown in Fig. 2. In the first iteration, a pentagon-shaped patch is designed and connected with a 50 Ω transmission line. In this iteration (step 1), the antenna resonates at 5.4 GHz with a wide bandwidth of 2.25 GHz (4.60–6.85 GHz) as illustrated in Fig. 3. The input impedance of 55.5 Ω is noted at 5.4 GHz, which shows sufficient impedance matching at this frequency. In the second iteration (step 2), two symmetrical hook-shaped resonators are attached to the upper side of the pentagonal shape as obvious from Fig. 2. The resonant frequency at 5.4 GHz is shifted to 4.24 GHz, while another resonance appears at 6.91 GHz. The first resonant band is shifted to a lower frequency side due to the increase in the electrical length of the main radiating part. Also, the hook-shaped radiator assists in the production of the second band at 6.91 GHz. In the second iteration (step 2), the antenna has 10 dB bandwidths of 1.11 GHz (3.73–4.84 GHz) and 900 MHz (6.4–7.3 GHz) for lower and higher bands, respectively as in Fig. 3. In the third iteration (Proposed Antenna), many changes are incorporated in the reported antenna in iteration two. In this iteration, a rectangular slot is inserted to the lower left side of the pentagon-shaped patch while two upper side slots are made in the patch. Additionally, the width of the hook-shaped strips is reduced as shown in Fig. 2. The changes made in the third iteration result in the shift of the first two resonances to the lower frequency side along with the production of the third frequency band at 8 GHz. The first two resonant bands are shifted towards lower frequency side due to the loading effects of the three slots. In this iteration, the antenna resonates at three frequencies centered at 3.5, 5.4, and 8 GHz. 10 dB bandwidths of 900 MHz,

800 MHz, and 1.6 GHz are noted for the first, second, and third resonant bands respectively as shown in Fig. 3.

2.1. Surface Current Distribution

The surface current distribution of the proposed antenna is shown in Fig. 4 for three resonant frequencies (3.5, 5.4, and 8 GHz). Fig. 4(a) shows the surface current distribution at 3.5 GHz. It can be well noted that maximum current is distributed on the inner edges of the symmetrical hook-shaped resonators while a uniform current is distributed on the whole surface of the pentagonal patch. It can be concluded from Fig. 4(a) that pentagonal patch and hook-shaped resonators are most important in adjusting the lower frequency band (3.5 GHz). Fig. 4(b) represents the surface current distribution on the antenna for 5.4 GHz. It can be noted that most of the current is concentrated on the hook-shaped resonator while a marginal current is symmetrically distributed on the upper left/right corner of the pentagonal patch. Also, some current contents are distributed uniformly on the lower side of the pentagonal patch. Hence, the middle resonance can be mainly controlled through the hook-shaped resonator. Fig. 4(c) shows the distribution of surface current on the patch as well as on the ground for the resonant frequency of 8 GHz. It is obvious from Fig. 4(c) that major content of the current is concentrated on the vertical slot while very lower content of the current is seen on the rest of the resonator. It can be well noted from this figure that the third resonance band can be controlled by changing the length and width of the vertical slot.

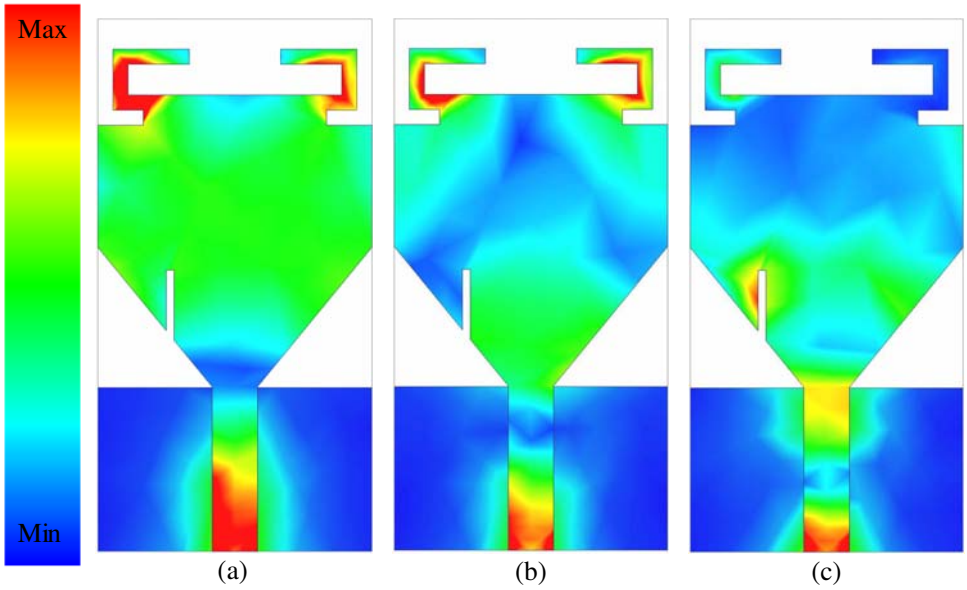

Figure 4. Surface current density (*Jsurf*) of the antenna at (a) 3.5 GHz, (b) 5.4 GHz, and (c) 8 GHz.

2.2. Parametric Analysis

The performance of the antenna in terms of its reflection coefficient against varying antenna's parameters is analyzed in this section. Fig. 5 illustrates the simulated reflection coefficient (S_{11}) against varying parameters L_2, L_1, and L_s. Fig. 5(a) shows the impact of changing parameter L_2 on the reflection coefficient of the antenna. As it is obvious from the surface current density graph (Fig. 4(a)), L_2 is effective in the first two resonant frequencies while it has a negligible impact on the higher resonant band. The resonant frequencies of the first and second resonant bands shift toward the lower frequency side for increasing L_2. The resonant frequency of the lower frequency band is noted at 3.5, 3.2, and 2.8 GHz for L_2 of 4, 5, and 6 mm, respectively. The resonant frequency of the lower frequency band is noted at 5.4, 5.3, and 5.15 GHz for L_2 of 4, 5, and 6 mm, respectively. The higher frequency band is

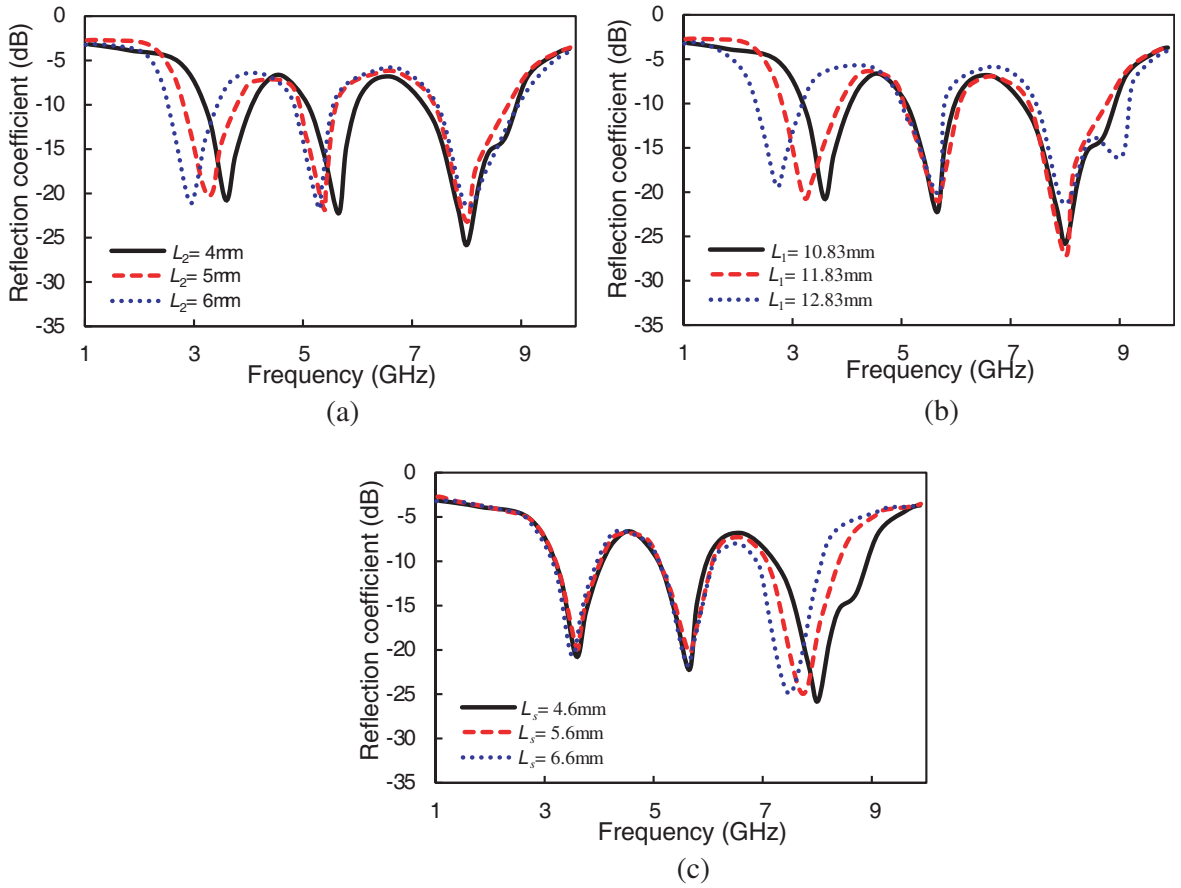

Figure 5. Reflection coefficient of the antenna against varying parameters (a) L_2, (b) L_1, and (c) L_s.

resistive toward any change in L_2. Fig. 5(b) shows the impact of varying parameter L_1 on the reflection coefficient of the antenna. It can be noted that increasing the parameter L_1 value results in shifting the lower frequency band to lower frequencies. Also, the remaining two resonant bands are resistive toward any change in parameter L_1 value. Fig. 5(c) shows the impact of varying L_s on the reflection coefficient of the antenna. The resonant frequency of the higher frequency band shifts towards lower frequency side by increasing the slot length (L_s).

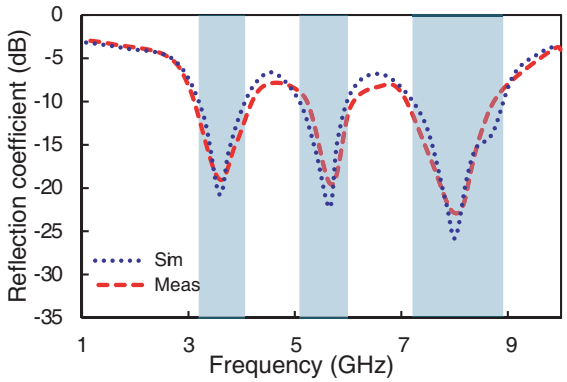

Figure 6. Simulated and measured reflection coefficient of the triple-band monopole antenna.

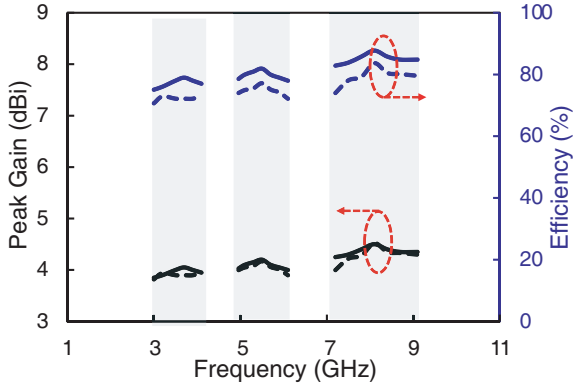

Figure 7. Simulated (solid line) and measured (dashed line) gain and efficiency.

3. RESULTS AND DISCUSSIONS

A prototype (Fig. 1(d)) of the simulated antenna is prepared in order to check its performance experimentally. 1.6 mm thicker FR-4 material is used for fabrication purposes.

3.1. Reflection Coefficient

The reflection coefficient of the proposed antenna (Fabricated prototype as shown in Fig. 1(d)) is measured using Vector Network Analyzer (VNA). The calibration of the VNA is performed using SOLT (short-open-load-through) technique. After calibrating the VNA, fabricated prototype is connected with VNA, and reflection coefficient is obtained. The simulated and measured results of the triple-band monopole antenna are presented in Fig. 6. A reasonable match between the simulated antenna's and fabricated antenna's results is observed. The simulated antenna has three resonant frequencies at 3.5, 5.4, and 8 GHz while the fabricated antenna has three resonant frequencies at 3.55, 5.59, and 8.05 GHz. Simulated 10 dB bandwidths of 900 MHz (3.2–4.1 GHz), 800 MHz (5.1–5.9 GHz), and 1.6 GHz (7.3–

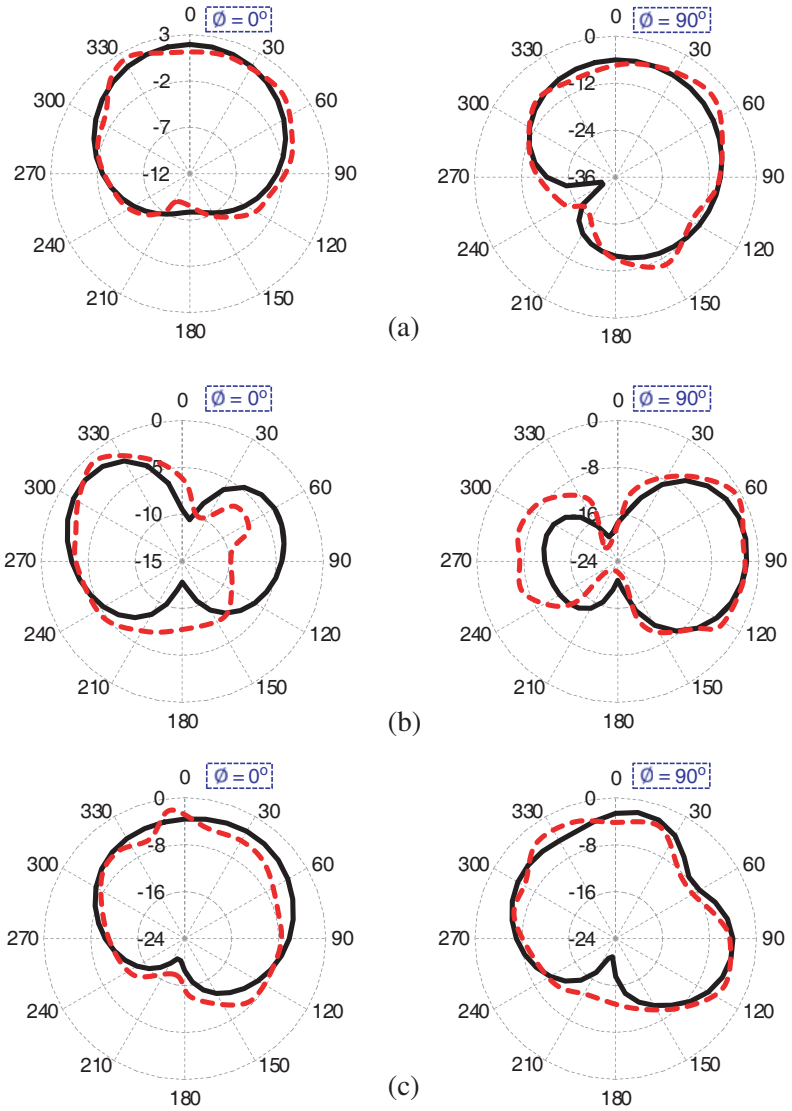

Figure 8. Simulated (solid line) and measured (dashed line) radiation pattern at (a) 3.5 GHz, (b) 5.4 GHz, and (c) 8 GHz.

Table 1. Comparison of proposed structure with those studied in literature.

Ref.	Size(mm^2)	Resonant Bands (GHz)	Bandwidths (MHz)	Gain (dBi)	Efficiency (%)	Controllable Bands
[1]	32×40	4.27	120	1.76	> 86	No
		4.85	160	2.3		
		6.45	250	1.45		
[2]	18×18	2.5	170	0.2	68	No
		3.47	100	0.16	56	
		5.75	280	0.62	72	
[3]	36×40	2.4	450	2.1	NG	No
		3.5	80	2		
		5.8	80	2.98		
[4]	40×30	2.4	120	1.66	66.8	No
		5.5	1100	4.75	83.6	
[6]	NG	2.35	90	6.72	83.2	No
		3.78	70	5.59	78.23	
		5.20	80	7.02	68.17	
[7]	38×25	2.61	300	1.85	NG	No
		3.5	1050	2.19		
		5.4	960	2.57		
[11]	40×35	2.45	140	2	NG	No
		5.2	2030	3.1		
[13]	70×50	1.8	430	NG	NG	No
		2.6	630			
		3.4	820			
This Work	**18×35**	**3.5**	**900**	**4**	**78**	**Yes**
		5.4	**800**	**4.2**	**79.95**	
		8	**1600**	**4.2**	**85.8**	

8.9 GHz) are observed for lower (WiMAX Band), middle (WLAN Band), and higher (X-Band) resonant bands, respectively. In the case of measured results, 10 dB band bandwidths of 930 MHz, 790 MHz, and 1.4 GHz are recorded for the lower, middle, and higher frequency bands, respectively.

3.2. Gain, Efficiency and Radiation Pattern

The fabricated antenna is experimentally tested for gain and efficiency. The simulated and measured results are compared in Fig. 7. The presented antenna has simulated gains of 4 dBi, 4.2 dBi, and 4.2 dBi at 3.5, 5.4, and 8 GHz, respectively. The antenna has simulated gain higher than 3.85 dBi, 4.03 dBi, and 4.15 dBi for the whole WiMAX, WLAN, and X-Band range. The measured gain of the fabricated antenna is recorded as 3.9 dBi, 4.17 dBi, and 4.22 dBi at 3.5, 5.4, and 8 GHz, respectively. The proposed antenna has simulated efficiency of 78%, 79.95%, and 85.8% at 3.5, 5.4, and 8 GHz, respectively, while a small reduction is reported for the measured efficiencies. The measured efficiencies of 72.15%, 77.2%, and 83% are recorded at 3.5, 5.4, and 8 GHz, respectively. The simulated and measured radiation patterns at both principal planes for three resonating frequencies are illustrated in Fig. 8. A very reasonable match is noted for simulated and measured results.

4. CONCLUSION

A low-profile triple-band monopole antenna for WiMAX, WLAN, and X-band applications is reported in this paper. The reported antenna works at three unique frequencies centered at 3.5 GHz, 5.4 GHz, and 8 GHz, covering absolute bandwidths of 900 MHz (3.2–4.1 GHz), 800 MHz (5.1–5.9 GHz), and 1.6 GHz

(7.3–8.9 GHz), respectively. This antenna possesses good gain and high efficiency at all operating bands. The presented antenna has simulated gains (efficiency) of 4 dBi (78%), 4.2 dBi (79.95%), and 4.2 dBi (85.8%) at 3.5, 5.4, and 8 GHz, respectively. The operating bands of the presented antenna can be tuned independently by varying certain correlated parameters. The hardware of the simulated antenna is successfully constructed and tested for validation of simulation results. A reasonable match between the simulated and measured results is observed at the operating bands in terms of the reflection coefficient, radiation pattern, gain, and efficiency.

Table 1 compares the performance of the proposed antenna with the antennas studied in the literature. It can be concluded from the comparison table that the proposed antenna has low profile, broad bandwidth, high gains and efficiencies compared to the antennas studied in the literature. One of the superior advantage of the proposed antenna over other antennas is its independently controllable bands.

REFERENCES

1. Iqbal, A., A. Bouazizi, O. A. Saraereh, A. Basir, and R. K. Gangwar, "Design of multiple band, meandered strips connected patch antenna," *Progress In Electromagnetics Research*, Vol. 79, 51–57, 2018.
2. Ali, T. and R. C. Biradar, "A triple-band highly miniaturized antenna for WiMAX/WLAN applications," *Microwave and Optical Technology Letters*, Vol. 60, No. 2, 466–471, 2018.
3. Chouti, L., I. Messaoudene, T. A. Denidni, and A. Benghalia, "Triple-band CPW-fed monopole antenna for wlan/wimax applications," *Progress In Electromagnetics Research*, Vol. 69, 1–7, 2017.
4. Sun, X. L., L. Liu, S. Cheung, and T. Yuk, "Dual-band antenna with compact radiator for 2.4/5.2/5.8 ghz wlan applications," *IEEE transactions on Antennas and Propagation*, Vol. 60, No. 12, 5924–5931, 2012.
5. Ghosh, A., V. Kumar, G. Sen, and S. Das, "Gain enhancement of triple-band patch antenna by using triple-band artificial magnetic conductor," *IET Microwaves, Antennas & Propagation*, Vol. 12, No. 8, 1400–1406, 2018.
6. Verma, M., B. Kanaujia, and J. Saini, "Design of fan-shaped stacked triple-band antenna for wlan/wimax applications," *Electromagnetics*, Vol. 38, No. 7, 469–477, 2018.
7. Pei, J., A.-G. Wang, S. Gao, and W. Leng, "Miniaturized triple-band antenna with a defected ground plane for wlan/wimax applications," *IEEE Antennas and Wireless Propagation Letters*, Vol. 10, 298–301, 2011.
8. Iqbal, A., S. Ullah, U. Naeem, A. Basir, and U. Ali, "Design, fabrication and measurement of a compact, frequency reconfigurable, modified t-shape planar antenna for portable applications," *Journal of Electrical Engineering & Technology*, Vol. 12, No. 4, 1611–1618, 2017.
9. Iqbal, A. and O. A. Saraereh, "A compact frequency reconfigurable monopole antenna for wi-fi/wlan applications," *Progress In Electromagnetics Research Letters*, Vol. 68, 79–84, 2017.
10. Boukarkar, A., X. Q. Lin, Y. Jiang, and Y. Q. Yu, "Miniaturized single-feed multiband patch antennas," *IEEE Transactions on Antennas and Propagation*, Vol. 65, No. 2, 850–854, 2017.
11. Song, Y., Y.-C. Jiao, H. Zhao, Z. Zhang, Z.-B. Weng, and F.-S. Zhang, "Compact printed monopole antenna for multiband WLAN applications," *Microwave and Optical Technology Letters*, Vol. 50, No. 2, 365–367, 2008.
12. Elavarasi, C. and T. Shanmuganantham, "SRR loaded CPW-fed multiple band rose flower-shaped fractal antenna," *Microwave and Optical Technology Letters*, Vol. 59, No. 7, 1720–1724, 2017.
13. Rahim, S. B. A., C. K. Lee, A. Qing, and M. H. Jamaluddin, "A triple-band hybrid rectangular dielectric resonator antenna (RDRA) for 4G LTE applications," *Wireless Personal Communications*, Vol. 98, No. 3, 3021–3033, 2018.